Rigorous results for tight-binding networks: Particle trapping and scattering

L. Jin and Z. Song*

School of Physics, Nankai University, Tianjin 300071, People's Republic of China

(Received 21 May 2009; published 10 February 2010)

We investigate the particle trapping and scattering properties in a tight-binding network, which consists of several subgraphs. The particle trapping condition is proved under which particles can be trapped in a subgraph without leaking. Based on exact solutions for the configuration of a π-shaped lattice, it is argued that the bound states in a specified subgraph are of two types, resonant and evanescent. We also link the result to the scattering problem. The scattering features of the π-shaped lattice is investigated in the framework of the Bethe ansatz.

DOI: 10.1103/PhysRevA.81.022107 PACS number(s): 03.65.−w, 73.22.Dj, 73.23.−b

I. INTRODUCTION

Trapping and scattering of a particle is an important feature in many quantum information processing systems. Due to the development of technology, the implementation of quantum information processing in quantum systems with periodic potentials such as optical lattices [1], arrays of quantum dots [2], photonic crystal [3], and coupled-resonator optical waveguide [4] has attracted intensive investigations. The design of quantum devices based on these promising technologies relies on the particle trapping and scattering properties in a discrete system. A heuristic example shows that the quantum confinement in a discrete system is distinct from its counterpart in continuum media [5] due to the Wannier-Stark localization [6].

This article focuses on noninteracting particles on a discrete lattice, which is treated by using the tight-binding approximation. Intuitively, the particle trapping is implemented by the sufficient strong on-site potential as the continuous system. In contrast to the continuum, however, different dynamical properties emerge in the lattice system due to its distinct dispersion relation. A local wave packet can be confined by the linear potential distribution [5] and the degree of spreading of a propagating wave packet can be controlled by the judicious choice of the particle energy [7–9]. Recent studies show that Fano resonance may be employed to construct the perfect mirror or transparency so as to control particles in a region of the lattice [10–12] via engineered configurations. Because of the numerous varieties of the possible geometry of the quantum network, we believe it is beneficial to have lattice-based exact solutions for the design of quantum devices. In this article, we rigorously show that the perfect particle trapping without any leakage can be achieved in simple tight-binding networks. This provides a method to devise the quantum network to confine particles with the required mode. We also link the results to the scattering problem. This general finding is illustrated by a practical network consisting of a waveguide with an embedded π-shaped subgraph. Exact solutions for such types of configurations are obtained to demonstrate and supplement the rigorous results.

*songtc@nankai.edu.cn

II. RIGOROUS RESULTS FOR PARTICLE TRAPPING

A general tight-binding network is constructed topologically by the sites and the various connections between them and is also represented as a vertex-edge graph. By cutting off some of the connections a graph is decomposed into several subgraphs. So when a particle is strictly trapped within a certain region of a network one can say that it is confined in a specified subgraph. The main aim of this article is to answer the questions of what kind of subgraphs can trap a particle as a bound state and of how such subgraphs scatter a particle when it is embedded in a waveguide. The Hamiltonian of a tight-binding network, or a graph that consists of n_0 subgraphs, reads as

$$\begin{aligned} H &= \sum_{l=1}^{n_0} H_l + \sum_{lm} H_{lm}, \\ H_l &= -\sum_{\langle ij\rangle} \left(\kappa_{ij}^{[l]} a_{l,i}^{\dagger} a_{l,j} + \text{H.c.}\right) + \sum_{i=1}^{N_l} \mu_i^{[l]} a_{l,i}^{\dagger} a_{l,i}, \\ H_{lm} &= -\sum_{i,j} \left(\kappa_{ij}^{[lm]} a_{l,i}^{\dagger} a_{m,j} + \text{H.c.}\right), \end{aligned} \tag{1}$$

where label l denotes the lth subgraph of the N_l site, the subgraph of which is defined by the distribution of the hopping integrals $\{\kappa_{ij}^{[l]}\}$ and the on-site potentials $\{\mu_i^{[l]}\}$ and $a_{l,j}^{\dagger}$ is the boson or fermion creation operator at the jth site in the lth subgraph. Here, H_l and H_{lm} represent the Hamiltonians of the subgraphs and the couplings between them. In terms of H_{lm}, site $i(j)$ is the *joint site* of subgraph $l(m)$ for the connections to the other subgraphs. Obviously, the decomposition of subgraphs is arbitrary and can be implemented at will. Figure 1 shows a schematical example. Note that the Hamiltonians H_l and H are quadratic in particle operators and can be diagonalized through the linear transformation

$$\eta_{l,k}^{\dagger} = \sum_j g_{k,j}^{l} a_{l,j}^{\dagger}, \tag{2}$$

which leads to

$$H_l = \sum_k \varepsilon_{l,k} \eta_{l,k}^{\dagger} \eta_{l,k}, \tag{3}$$

where $\varepsilon_{l,k}$ is the corresponding eigenvalue of H_l for the eigenfunction $g_{k,j}^{l}$. Site j is defined as the wave node for

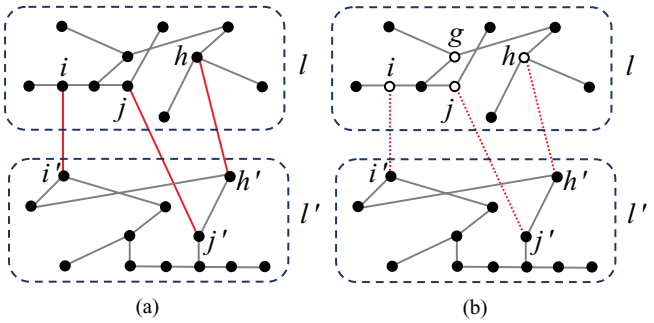

FIG. 1. (Color online) An arbitrary graph of a tight-binding network within part of which particles may be confined without any leakage. (a) The graph can be decomposed into two subgraphs l and l', which are connected via the coupling between the joint sites (i, j, h) and (i', j', h'). (b) The perfect bound states can be formed in subgraph l when the eigen functions of H_l have wave nodes on all the joint sites (i, j, h), which are denoted by empty circles. The existence of more wave nodes (as in site g) may allow multiple bound states.

the eigenmode k of graph l if we have $g^l_{k,j} = 0$. We denote the wave node as $j(l, k)$, which reflects the property of the eigenstate $\eta^\dagger_{l,k}|0\rangle$ of H_l

$$a_{l,j}\eta^\dagger_{l,k}|0\rangle = 0, \tag{4}$$

where $|0\rangle$ is the vacuum state. Now we consider the case that *all* the joint sites of the subgraph l are the wave nodes of eigenmode k. Under this condition, we have

$$H(\eta^\dagger_{l,k}|0\rangle) = H_l(\eta^\dagger_{l,k}|0\rangle) = \varepsilon_{l,k}(\eta^\dagger_{l,k}|0\rangle), \tag{5}$$

that is, the eigenstate $\eta^\dagger_{l,k}|0\rangle$ is also the eigenstate of the whole graph H. Then such a state represents the trapping or bound state of a particle within the subgraph l with infinite lifetime. This rigorous conclusion has important implications in the design of a quantum network to store particles in the target region at will. Figure 1 represents an arbitrary graph of a tight-binding network within part of which particles can be confined without any leakage. The whole graph can be decomposed into two subgraphs l and l', which are connected via the couplings between the joint sites (i, j, h) and (i', j', h'). The perfect bound state can be formed in subgraph l as the eigenfunction of H_l when it has wave nodes on all the joint sites (i, j, h). The existence of additional wave nodes indicates that the multiple bound states can be formed.

III. DEMONSTRATION CONFIGURATIONS

Now we investigate a class of practical examples to demonstrate the application of the previous result. We consider a system of a π-shaped lattice (Fig. 2), consisting of an infinite chain side coupling to two finite chains of length N_0 at the joint sites 1 and L, which has the Hamiltonian

$$\begin{aligned} H &= H_a + H_b + H_c + H_{\text{joint}}, \\ H_a + H_b &= -\kappa_0 \sum_{i=1}^{N_0} (a_i^\dagger a_{i+1} + b_i^\dagger b_{i+1} + \text{H.c.}), \\ H_c &= -\kappa \sum_{i=-\infty}^{\infty} (c_i^\dagger c_{i+1} + \text{H.c.}), \end{aligned} \tag{6}$$

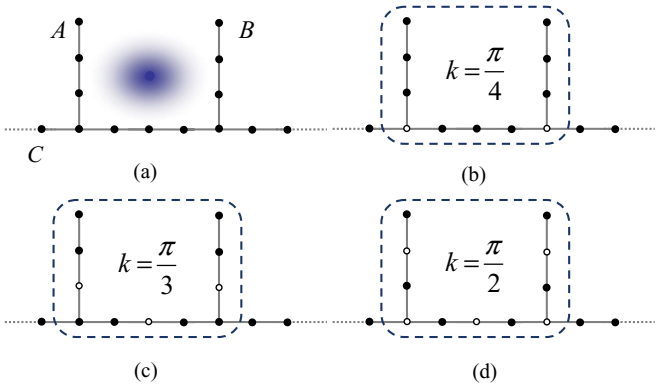

FIG. 2. (Color online) Configuration of a π-shaped lattice that admits the formation of trapping particles. It consists of three chains A, B, and C. (a) Two three-site chains A and B are side coupled to the chain C with an arbitrary number of sites. This graph can be decomposed into three subgraphs, one of which is an 11-site chain enclosed by the dashed rectangle. The single-particle eigen states of the 11-site chain with quasimomenta $k = \pi/4$, $\pi/3$, and $\pi/2$ have two, three, and four wave nodes, denoted by the empty circles in (b), (c), and (d). For states with $k = \pi/4$ and $\pi/2$, the joint sites being all wave nodes, the particle can be trapped in the 11-site chain, while a state with $k = \pi/3$ is not a bound state. States with other values of k can be analyzed accordingly.

$$H_{\text{joint}} = -\kappa_0(a_1^\dagger c_1 + b_1^\dagger c_L + \text{H.c.}),$$

where $a_j^\dagger$ ($b_j^\dagger$ and $c_j^\dagger$) is the boson or fermion creation operator at the jth site in the chain a (b and c). The side coupling model was employed to depict the coupled-cavity system for stopping and storing light coherently [13]. For the simple case with the shortest side chains, $N_0 = 1$, the configuration is equivalent to the atom-cavity system with single excitation [10,11] where the side-site state represents the excited state of the two-level atom.

First of all, we consider a simplest case: The hopping integrals are identical for all chains $\kappa = \kappa_0$. This graph can be decomposed into three subgraphs: left chain, right chain, and central chain of $\Lambda = 2N_0 + L$ sites. The eigenfunctions of the central chain are given by

$$g_{k,j} = \sqrt{\frac{2}{\Lambda + 1}} \sin kj, \quad j \in [1, \Lambda], \tag{7}$$

where $k = n\pi/(\Lambda + 1), n \in [1, \Lambda]$, with corresponding eigenvalues $-2\kappa \cos k$. These states possess the wave nodes at

$$j_k = \frac{(\Lambda + 1)m}{n}, \tag{8}$$

where m are certain integers that ensure the existence of integer j_k for a given n. Then, in the case that $\{j_k\}$ covers the joint sites $N_0 + 1$ and $N_0 + L$ simultaneously, the corresponding eigenstates are the trapping states and a particle can be held along the central chain indefinitely. An example of $N_0 = 3$, $L = 5$ is depicted in Fig. 2, where only typical cases with $k = \pi/4, \pi/3$, and $\pi/2$ are presented. Actually, Eq. (8) shows that states with $k = \pi/4$, $\pi/2$, and $3\pi/4$ have wave nodes at the joint sites. Therefore, there are three resonant bound states for this configuration. It was proposed that such a kind of trapping state can act as a cavity when a boson system

is considered [11]. Remarkably, two peculiar features are identified. First, the bound state has infinite lifetime in the ideal case without decoherence since it is based on the mechanism of Fano interference rather than two potential barriers. Second, the number of the cavity mode does not solely depend on the size of the cavity L as in the case of using an infinite potential well for particle trapping. For example, taking $N_0 = 1$, one can achieve a single mode cavity with $k = \pi/2$ for arbitrary odd L but none for even L. Meanwhile, it will be shown later that there is another type of bound state, *evanescent* bound state. Besides these exact bound states, there exist eigenstates of the subgraph that have nonzero, but very small probability at the joint sites in the case of large L. Such kinds of states have finite but long lifetimes, which are called quasiresonant bound states. To demonstrate these concepts we present a numerical simulation of the damping process for various modes in two typical systems with $N_0 = 2$, $L = 4$ and $N_0 = 3$, $L = 123$, respectively. A particle is initially located in the subgraph in the eigenstates $|k\rangle$ [Eq. (7)]. We investigate the dynamics of the states by computing the quantity

$$P(k,t) = \left\langle \sum_{i=1}^{N_0} (a_i^\dagger a_i + b_i^\dagger b_i) + \sum_{i=1}^{L} c_i^\dagger c_i \right\rangle_{k,t}, \qquad (9)$$

where $\langle \ldots \rangle_{k,t}$ denotes the expectation value of the probability of the particle within the subgraph for an evolved state $\exp(-iHt)|k\rangle$. Figure 3 shows the numerical simulation of $P(k,t)$ as functions of the mode k and time t for a short L in the upper plot while for a longer L in the lower plot. There are three types of curves in the two plots: (i) remaining unitary; (ii) damping slowly; and (iii) dropping drastically and then keeping at a finite value. Case (i) occurs in both configurations, corresponding to the perfect resonant bound states. Case (ii) occurs in the large-L system, corresponding to the quasiresonant bound state (we omit such a type of curve in the lower panel). Case (iii) occurs in the small-L system, corresponding to another type of bound state, the evanescent bound state, which will be discussed in detail later.

A resonant bound-state configuration can be understood from the point of view of interference. The bound state we constructed in this manner is the standing-wave-like state in the subgraph. In general, the formation of a standing wave in a quantum system is due to the infinite potential barriers that reflect the wave with *any* momentum. Then there is no additional condition for the distance between the two barriers. In a tight-binding network, a side coupled chain can act as the infinite potential barriers for the incident wave with *certain* momentum. As an example, it can be readily shown by the following method that for an incident wave with $k = \pi/2$, the transmission coefficient T through one side coupled chain of length N_0 can be expressed as $T = [1 + (-1)^{N_0}]/2$. This was discussed in Refs. [10,11] for the case of $N_0 = 1$. Besides the mirror condition $T = 0$, a matching distance between the two side coupled chains is also required to form a standing wave. This will be discussed in the following in the aid of exact results.

In the previous analysis, the trapping subgraph is the simplest lattice, an open chain. There are some more complicated subgraphs, the hierarchical lattices, as the demonstration configurations. It was shown that [14–16] there are eigenfunctions

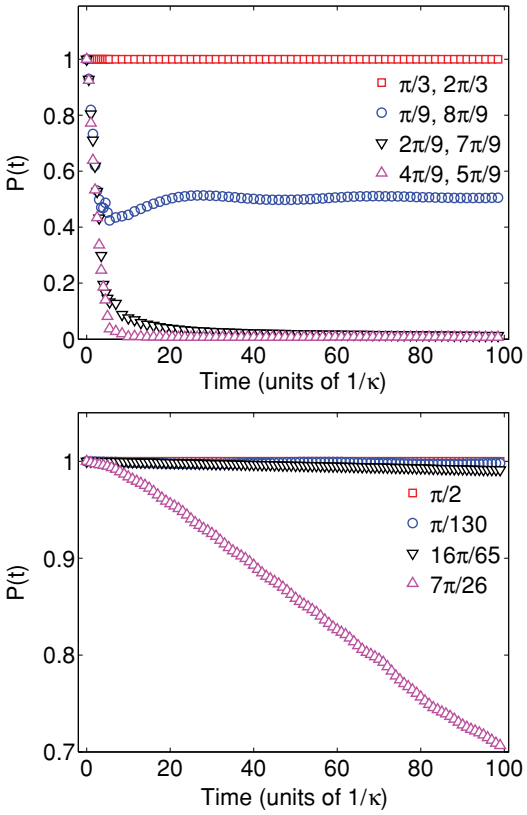

FIG. 3. (Color online) The probability $P(k,t)$ of a particle, initially located in the state $|k\rangle$, remaining in the subgraph. The simulations are performed in two typical systems with $N_0 = 2$, $L = 4$ (upper panel) and $N_0 = 3$, $L = 123$ (lower panel), respectively. The shapes of all the curves can be classified into three types as mentioned in the text.

of these hierarchical lattices, the amplitudes of which are zero at certain sites. When these lattices are embedded in a network by linking the nodes only the trapping states are formed. Considering an arbitrary generation Vicsek fractal as an example, there is an eigenfunction the amplitude of which is zero at the center of every five-site cell. Then, when such a lattice is embedded in a network by linking the center sites only, the corresponding eigenstate is the trapping state with respect to the network. Nevertheless, for the hierarchical lattice itself this eigenstate becomes an extended state as its size increases.

IV. BETHE-ANSATZ RESULTS

We now turn to discussing the complete bound states in a subgraph by taking the network of Eq. (6) as an example. It is worth pointing out that the bound states constructed by the previously mentioned method are not complete. In the following it will be shown that there are two types of bound states: *resonant* and *evanescent*. The former describes a trapped particle in a specified spatial region and the later describes a particle with an exponentially decaying probability beyond a specified spatial region. In the following, we investigate this problem based on the Bethe-ansatz approach. Actually, the bound-state wave functions $\psi(j)$ of the Hamiltonian (6) can be expressed as a

piecewise function over all sites

$$\psi_c(j)=\begin{cases} C_1e^{-ik(j-1)} & \text{for} \quad j\leqslant 1,\\ C_2e^{ikj}+C_3e^{-ikj} & \text{for} \quad 2\leqslant j<L,\\ C_4e^{ik(j-L)} & \text{for} \quad j\geqslant L,\end{cases}$$

$$\psi_a(j)=A_1e^{iqj}+A_2e^{-iqj} \quad \text{for} \quad 1\leqslant j\leqslant N_0,$$

$$\psi_b(j)=B_1e^{iqj}+B_2e^{-iqj} \quad \text{for} \quad 1\leqslant j\leqslant N_0.$$

Here $\psi_{a,b,c}$ denote the wave functions along chains a, b, and c, respectively. The coefficients and momenta $C_{1,2,3,4}$, $A_{1,2}$, $B_{1,2}$, k, and q are determined by matching conditions and the corresponding Schrödinger equations [17]

$$\psi(j+0^+)=\psi(j+0^-), \tag{10}$$

$$-\kappa_{j+1,j}\psi(j+1)-\kappa_{j-1,j}\psi(j-1)=E\psi(j), \tag{11}$$

where E is the eigen energy and $\kappa_{j\pm1,j}$ are the corresponding hopping integrals. The solutions can be classified in two categories: *resonant* and *evanescent*, which correspond to zero and nonzero $C_{1,4}$, respectively.

For the resonant bound states, zero $C_{1,4}$ leads to zero particle probability at the joint points, which is consistent with the previously mentioned results. In addition, the momenta k and q are determined by equations

$$\sin[k(L-1)]=\sin[q(N_0+1)]=0, \tag{12}$$

$$E=-2\kappa_0\cos q=-2\kappa\cos k. \tag{13}$$

For simplicity, only simple cases with $\kappa_0=\kappa$ are considered to demonstrate and explore the obtained results. The existence of the solution requires $(L-1)m=(N_0+1)n$, where $n\in[1,L-2]$ and $m\in[1,N_0]$. Obviously, the resonant bound states in the previously mentioned example with $N_0=3$ and $L=5$ are the simplest case of $m=n=1$, 2, and 3, corresponding to momenta $\pi/4$, $\pi/2$, and $3\pi/4$, respectively.

For the evanescent bound state, which possesses nonzero particle probability at and around the joint points, the momenta k and q are determined by equations

$$\frac{\kappa\zeta(k)}{\zeta(k(L-1))}[e^{-ik(L-1)}\pm1]=\frac{\kappa_0\zeta(qN_0)}{\zeta(q(N_0+1))}, \tag{14}$$

$$E=-2\kappa_0\eta(q)=-2\kappa\eta(k), \tag{15}$$

where $\zeta(\theta)=(e^{i\theta}-e^{-i\theta})/2$ and $\eta(\theta)=(e^{i\theta}+e^{-i\theta})/2$. Taking $\kappa_0=\kappa$, $N_0=3$, and $L=5$ as an example, we have $q=k=0.382i$, $\pi+0.382i$, or $0.191i$, $\pi+0.191i$, which correspond to symmetric and antisymmetric evanescent bound eigenfunctions, respectively. Furthermore, for the case of $\kappa_0=\kappa$, $N_0=2$, and $L=4$, plotted in Fig. 3, we have $q=k=0.382i$ or $\pi+0.382i$. Accordingly, three initial states with momenta $\pi/9$, $2\pi/9$, and $4\pi/9$, as well as their counterparts have nonzero overlaps with the two evanescent bound states. We are then able to obtain the long-time behaviors of $P(t)$ as 0.5032, 0.0027, and 0.0058, which are in agreement with the plots in the upper panel of Fig. 3.

V. SCATTERING PROBLEMS

In general, trapping and scattering are two contrary phenomena, which always refer to localized and extended states. In the context of this article, the resonant bound state is essentially standing-wave-like, consisting of two constituents: incident and reflected waves. On the other hand, the result for such bound states has no restriction to the size and geometry of the subgraph and is applicable to the scattering problem. This is another main issue we want to stress in this article.

For the scattering problem, the input-output waveguides and the center system should be involved. One can take the input waveguide, which is usually a semi-infinite chain, together with a part of the center system as the subgraph. The resonant bound state in such a subgraph corresponds to a total reflection. Actually, the trapping wave function within the input waveguide region is the superposition of two opposite traveling plane waves with identical amplitudes. They correspond to the incident and total reflected waves and the eigen energy E of this trapping state is exactly the transmission zero, $T(E)=0$. Taking the previous π-shaped lattice as an illustrated example, the subgraph containing the input waveguide is depicted by the Hamiltonian

$$H_{\text{in}}=-\kappa\left(\sum_{i=1}^{N_0}a_i^\dagger a_{i+1}+a_1^\dagger c_1+\sum_{i=-\infty}^{1}c_i^\dagger c_{i+1}+\text{H.c.}\right), \tag{16}$$

which is a uniform semi-infinite chain. The resonant bound states must have a node at site c_1 with energy $E=-2\kappa\cos q$, where q is determined by the position of the node $\sin[q(N_0+1)]=0$.

Now we consider the scattering problem of the π-shaped lattice, demonstrating the relation linking the scattering state and resonant bound state in the framework of the Bethe ansatz. It is worth noting that much effort was devoted to discussing critically the effect of a dangling side coupled chain on the spectrum and transmission properties of a linear chain, including the Fano resonance, by approximate approaches [18–21].

In a π-shaped lattice, the scattering wave function has the form

$$\psi_c(j)=\begin{cases} e^{ik(j-1)}+re^{-ik(j-1)} & \text{for} \quad j\leqslant 1,\\ Ae^{ik(j-1)}+Be^{-ik(j-1)} & \text{for} \quad 2\leqslant j<L,\\ te^{ik(j-1)} & \text{for} \quad j\geqslant L,\end{cases}$$

$$\psi_a(j)=C_ae^{iqj}+D_ae^{-iqj}, \quad \text{for} \quad 1\leqslant j\leqslant N_0,$$

$$\psi_b(j)=C_be^{iqj}+D_be^{-iqj}, \quad \text{for} \quad 1\leqslant j\leqslant N_0,$$

where r and t are the reflection and transmission amplitudes for an incident wave with momentum k. Similarly, applying the matching conditions [Eq. (10)] and the corresponding Schrödinger equations [Eq. (11)], we then obtain

$$t=\frac{\alpha^2\sin^2k}{\alpha^2\sin^2k-i\alpha\beta\sin k+(\beta/2)^2[e^{i2k(L-1)}-1]}, \tag{17}$$

where $\alpha=\kappa\sin[q(N_0+1)]$ and $\beta=\kappa_0\sin(qN_0)$. Note that zero α leads to the vanishing of t, while zero β leads to the vanishing of r. The former and latter are in agreement with the conclusions of the previous analysis from the interference point of view for the total reflection and resonant transmissions, respectively.

From Eq. (17), the transmission probability has the form

$$T=\frac{\alpha^4\sin^4k}{\alpha^4\sin^4k+(\beta/2)^2(\beta^2+4\alpha^2\sin^2k)\sin^2[k(L-1)-\delta]}, \tag{18}$$

where $\tan\delta = 2\alpha \sin k/\beta$. Equation (18) allows the analytical investigation on the transmission features. First, it is found that the total reflection condition coincides with the resonant bound condition Eq. (12). It indicates the conclusion that an incident wave is totally reflected by the side coupled chains if its energy is exactly equal to the resonant bound-state energy. The same conclusion was obtained for some similar systems [18–21]. This is a direct result from the fact that the scattering of any dangling side coupled chain is isotropic for the incident waves from both sides along the waveguide. On the other hand, the resonant transmission condition is also easy to understand from the aspect of wave nodes in the subgraph. In fact equation $\sin(qN_0) = 0$ indicates the effective disconnection of the wave guide from the side coupled system.

Second, for a fixed N_0, the common transmission zeros and reflection zeros for arbitrary L can be simply determined by $\alpha = 0$ and $\beta = 0$, respectively. More precisely, for the incident waves with $k_{\min} = \cos^{-1}\{(\kappa_0/\kappa)\cos[n\pi/(N_0+1)]\}$, $n \in \mathbb{Z}$, we have $T = 0$, while the one with $k_{\max} = \cos^{-1}[(\kappa_0/\kappa)\cos(n\pi/N_0)]$, we have $T = 1$. The rest reflection zeros are L dependent and determined by $\sin^2[k(L-1) - \delta] = 0$.

The transmission spectra are plotted for $\kappa = \kappa_0$, $N_0 = 2$, 3, and different L in Fig. 4 as illustration. We can see that the common transmission zeros occur at $E = -1$ for $N_0 = 2$; $E = -\sqrt{2}$ for $N_0 = 3$, while the common reflection zeros occur at $E = 0$ for $N_0 = 2$; $E = -1$ for $N_0 = 3$, which are in agreement with the earlier analysis. From the plots, one can find that it does not exhibit a perfect Fano line shape. Nevertheless, the peak and dips profiles are the direct result of an interference result from subwaves in different paths. Actually, the formations of $k_{\min}$ and $k_{\max}$ correspond to the complete destructive and constructive interferences.

Now we focus on the L-dependent reflection zeros. Consider a system with fixed $L = L_0$, the L-dependent reflection zeros occur at k_0, which satisfies

$$\sin^2[k_0(L_0 - 1) - \delta] = 0. \tag{19}$$

Meanwhile, for a system with $L = L_0 + m$, the corresponding transmission coefficient obeys

$$T(k_0, L_0 + m) = T(k_0, L_0 - m), \tag{20}$$

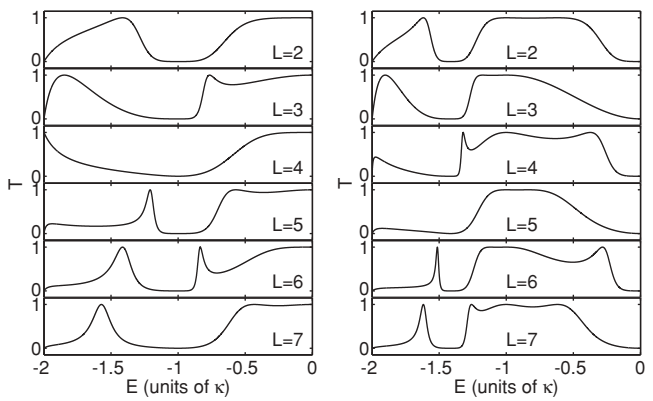

FIG. 4. The plots of $T(E)$ from Eq. (18) for the systems of $N_0 = 2$ (left) and 3 (right) with different L.

for $L_0 - m \succ 0$, due to the identity

$$\sin^2[k_0(L_0 + m - 1) - \delta] = \sin^2(mk_0). \tag{21}$$

This fact leads to an interesting conclusion. For a certain k_0, if there are two systems L and L' that satisfy $T(k_0, L) = T(k_0, L') = 1$, there should exist a series of different L, L', L'', L''', . . . , to satisfy $T(k_0, L'') = T(k_0, L''') = \cdots = 1$. Especially applying this conclusion for the $m = 1$ case, it follows that there is no k_0 to satisfy $T(k_0, L) = T(k_0, L+1) = 1$, except the common reflection zeros. In other words, there are no L-dependent reflection zeros for L and $L+1$ meeting at the same k. This feature enhances the probability of the occurrence of the so-called peak-dip swapping as L changes [20,21].

For a fixed N_0, one can always find two systems with successive L that have at least one peak (reflection zero) located at each side of a common dip (transmission zero). Since there is only one peak at each k_0, the peak-dip swapping profile is formed in the vicinity of a common dip. Here we exemplify this point by investigating the cases with $\kappa = \kappa_0$ and small N_0. For $N_0 = 2$, one of the common transmission zero is $k_{\min} = \pi/3$, while the L-dependent reflection zeros are determined by $\sin^2[k_0(L_0 - 1) - \delta] = 0$. The closest (or closer) solution of k_0

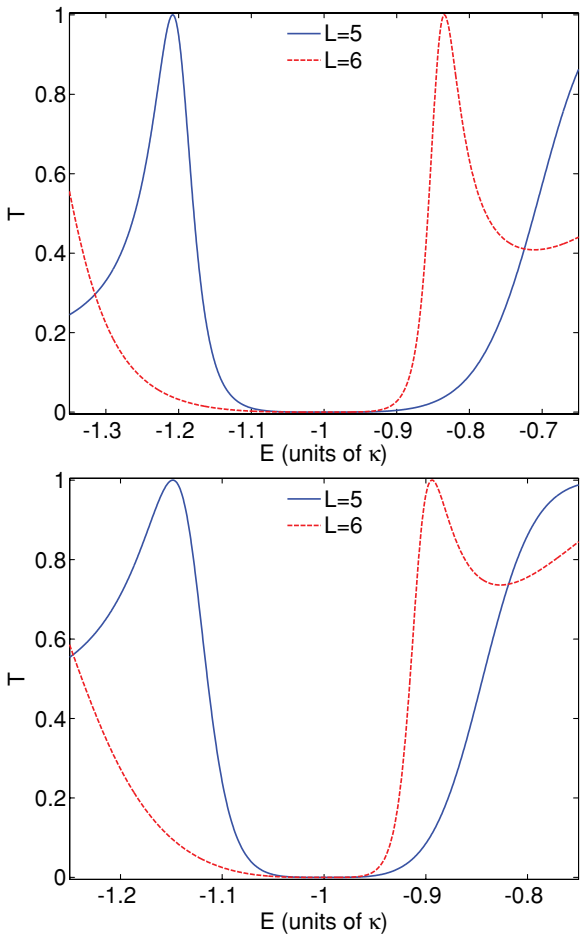

FIG. 5. (Color online) Transmission probability $T(E)$ for the configurations with $N_0 = 2$ (up panel), 5 (down panel), and $L = 5$ (solid blue line), $L = 6$ (dashed red line). The plots show the evident swapping of peak-dip profiles.

around $k_{\min} = \pi/3$ is the left one $k_{0L} = 0.29\pi$ $(E = -1.21)$ for $L = 5$ and the right one $k_{0R} = 0.36\pi$ $(E = -0.84)$ for $L = 6$. The profiles of the corresponding transmission spectra are plotted in Fig. 5 (upper), which exhibit the same character as the one in Fig. 7 of Ref. [20]. Another example for $N_0 = 5$ and $L = 5, 6$ is also plotted in Fig. 5 (lower). One can see the occurrence of the profile of the evident peak-dip swapping.

VI. SUMMARY

In summary, we show in this article within the context of a tight-binding model that a particle can be trapped in a nontrivial subgraph. As an application, we examine concrete networks consisting of a π-shaped lattice. Exact solutions for such types of configurations are obtained to demonstrate and supplement the results. It is shown that there are two types of bound states: resonant and evanescent. We also link the results to the scattering problem for such a subgraph being embedded in a one-dimensional chain as the waveguide. It is shown that an incident wave experiences total reflection under a certain condition. Finally, we also investigate the scattering features of the π-shaped lattice in the framework of the Bethe ansatz. Such results are expected to be necessary and insightful for quantum control and engineering.

ACKNOWLEDGMENTS

We acknowledge the support of the CNSF (Grant Nos. 10874091 and 2006CB921205).

[1] O. Mandel, M. Greiner, A. Widera, T. Rom, T. W. Hänsch, and I. Bloch, Nature (London) **425**, 937 (2003).
[2] B. E. Kane, Nature (London) **393**, 133 (1998); D. Loss and D. P. DiVincenzo, Phys. Rev. A **57**, 120 (1998).
[3] J. Bravo-Abad and M. Soljačić, Nat. Mater. **6**, 799 (2007); Y. Tanaka, J. Upham, T. Nagashima, T. Sugiya, T. Asano, and S. Noda, *ibid.* **6**, 862 (2007).
[4] M. Sandberg, C. M. Wilson, F. Persson, T. Bauch, G. Johansson, V. Shumeiko, T. Duty, and P. Delsing, Appl. Phys. Lett. **92**, 203501 (2008); M. A. Castellanos-Beltran and K. W. Lehnert, *ibid.* **91**, 083509 (2007).
[5] S. Longhi, Phys. Rev. E **75**, 026606 (2007).
[6] H. Fukuyama, R. A. Bari, and H. C. Fogedby, Phys. Rev. B **8**, 5579 (1973).
[7] T. J. Osborne and N. Linden, Phys. Rev. A **69**, 052315 (2004).
[8] S. Yang, Z. Song, and C. P. Sun, Phys. Rev. A **73**, 022317 (2006).
[9] W. Kim, L. Covaci, and F. Marsiglio, Phys. Rev. B **74**, 205120 (2006).
[10] L. Zhou, Z. R. Gong, Y. X. Liu, C. P. Sun, and F. Nori, Phys. Rev. Lett. **101**, 100501 (2008).
[11] L. Zhou, H. Dong, Y. X. Liu, C. P. Sun, and F. Nori, Phys. Rev. A **78**, 063827 (2008).
[12] J. Q. Liao, J. F. Huang, Y. X. Liu, L. M. Kuang, and C. P. Sun, Phys. Rev. A **80**, 014301 (2009).
[13] M. F. Yanik and S. H. Fan, Phys. Rev. Lett. **92**, 083901 (2004); Phys. Rev. A **71**, 013803 (2005).
[14] Z. Lin and M. Goda, J. Phys. A **26**, L1217 (1993).
[15] A. Chakrabarti and B. Bhattacharyya, Phys. Rev. B **54**, R12625 (1996).
[16] A. Chakraborti, B. Bhattacharyya, and A. Chakrabarti, Phys. Rev. B **61**, 7395 (2000).
[17] J. E. Hirsch, Phys. Rev. B **50**, 3165 (1994).
[18] A. E. Miroshnichenko and Y. S. Kivshar, Phys. Rev. E **72**, 056611 (2005).
[19] P. A. Orellana, F. Domínguez-Adame, I. Gómez, and M. L. Ladrón de Guevara, Phys. Rev. B **67**, 085321 (2003).
[20] A. Chakrabarti, Phys. Rev. B **74**, 205315 (2006).
[21] A. Chakrabarti, Phys. Lett. **A366**, 507 (2007).